Earth and Planetary Science Letters 368 (2013) 144–150

Contents lists available at SciVerse ScienceDirect

Earth and Planetary Science Letters

journal homepage: www.elsevier.com/locate/epsl

# Long-term changes of earthquake inter-event times and low-frequency earthquake recurrence in central California

Chunquan Wu [a,*], David R. Shelly [b], Joan Gomberg [c], Zhigang Peng [d], Paul Johnson [a]

[a] Geophysics Group, Los Alamos National Laboratory, Los Alamos, NM 87545, USA
[b] US Geological Survey, Menlo Park, CA 94025, USA
[c] US Geological Survey, Seattle, WA 98195, USA
[d] School of Earth and Atmospheric Sciences, Georgia Institute of Technology, Atlanta, GA 30332, USA

ARTICLE INFO

*Article history:*
Received 14 December 2012
Received in revised form
6 March 2013
Accepted 7 March 2013
Editor: P. Shearer

*Keywords:*
nonvolcanic tremor
low-frequency earthquake
Parkfield earthquake
long-term changes
episodic tremor and slip
central California

ABSTRACT

The temporal evolution of earthquake inter-event time (IET) may provide important clues for the timing of future events and underlying physical mechanisms of earthquake interaction. In this study, we examine ~12 yr of local earthquake and low-frequency earthquake (LFE) activity near Parkfield, CA from catalogs of ~50,000 earthquakes and ~730,000 LFEs. We focus on the long-term evolution of IETs after the 2003 Mw6.5 San Simeon and 2004 Mw6.0 Parkfield earthquakes. The IETs of local earthquakes along and to the southwest of the San Andreas fault show clear decreases of several orders of magnitude after the Parkfield and San Simeon earthquakes, followed by recoveries with time scales of ~3 yr and $>8$ yr, respectively. We also observe decreases in recurrence times in some of LFE families, followed by long-term recoveries with time scales of ~4 months to several years. The long-term recovery of the earthquake IET is a manifestation of the aftershock decay of the Parkfield and San Simeon earthquakes, and the different recovery time scales likely reflect the different tectonic loading rates in the two regions. The drop in the recurrence times of LFEs after the Parkfield earthquake is likely caused by static and dynamic stresses induced by the Parkfield earthquake, and the long-term recovery in LFE recurrence time could be due to post-seismic relaxation or gradual recovery of fault zone material properties. The recovery time scales for general earthquake IET and LFE recurrence following the Parkfield earthquake are similar to those estimated for repeating earthquake recurrence identified in previous studies, indicating that they could be controlled by similar mechanisms.



## 1. Introduction

Stress changes induced by large earthquakes can affect seismicity rates at both close and far distances (e.g., Stein, 1999; Hill and Prejean, 2007, and references therein). Recent studies have also inferred that the stresses from nearby or remote earthquakes may cause both transient and longer-term changes in the behavior of non-volcanic tremor (e.g., Gomberg et al., 2008; Nadeau and Guilhem, 2009; Peng et al., 2009; Shelly et al., 2011; Chao et al., 2012; Guilhem and Nadeau, 2012), which may be considered as swarms of low-frequency earthquakes (LFEs) that reflect shear slip on the deeper fault interface (Shelly et al., 2007). LFEs may provide important clues about deep fault slip in the lower crust (Rubinstein et al., 2010) and future earthquake occurrence (Shelly, 2009, 2010a).

The December 22, 2003 Mw6.5 San Simeon (McLaren et al., 2008) and the September 28, 2004 Mw6.0 Parkfield earthquakes (Bakun et al., 2005) are the largest earthquakes in central California (Fig. 1) since continuous archiving of waveforms from the High Resolution Seismic Network (HRSN) began in 2001. Several recent studies have investigated stress changes induced by the San Simeon and Parkfield earthquakes and the resultant changes in the seismicity and LFE rates (e.g., Aron and Hardebeck, 2009; Lengline and Marsan, 2009; Chen et al., 2010; Shelly and Johnson, 2011). These studies found that both the San Simeon and Parkfield earthquakes caused significant changes in the rates of regular earthquakes and LFEs. However, most previous studies focused on the variations in the spatial distributions and short-term seismicity rates surrounding the two large earthquakes. A detailed investigation of the longer-term (months to years) temporal evolution after the two large earthquakes is important for better understanding the loading and stressing condition of the fault system, deep fault creep, and post-seismic recovery of fault zone material properties (e.g., Brenguier et al., 2008; Rubinstein et al., 2010).

* Corresponding author. Tel.: +1 505 665 0525.
*E-mail addresses:* chunquanwu@gmail.com, cwu@lanl.gov.(C. Wu)

0012-821X/$ - see front matter © 2013 Elsevier B.V. All rights reserved.
http://dx.doi.org/10.1016/j.epsl.2013.03.007

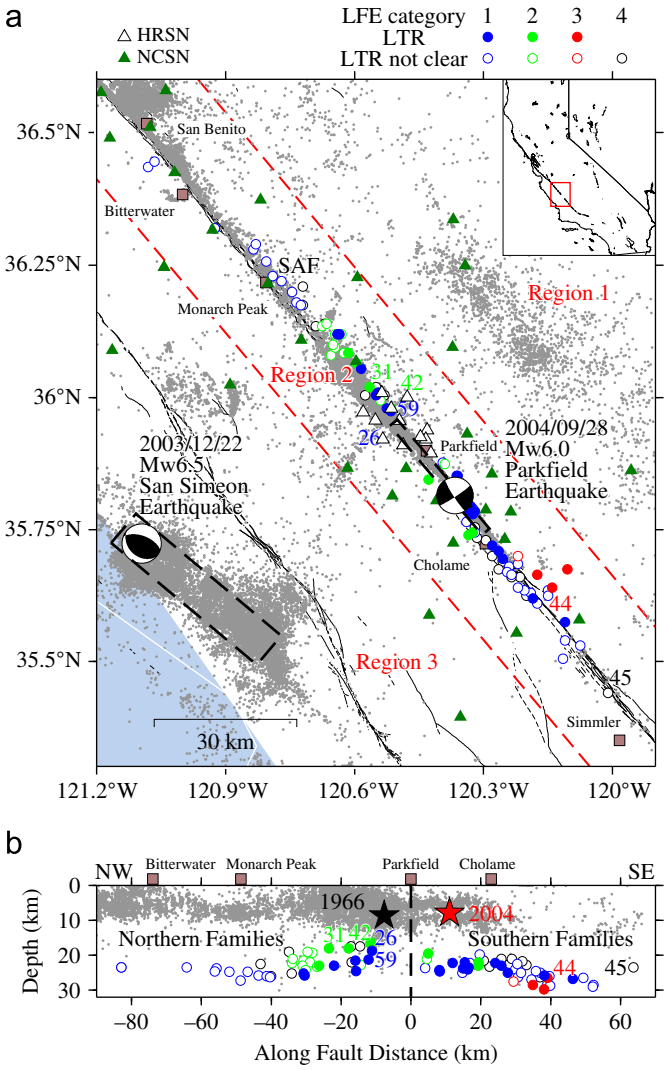


**Fig. 1.** (a) Map of the study region in Parkfield, CA. The epicenters of the 2003 Mw6.5 San Simeon earthquake and 2004 Mw6.0 Parkfield earthquake are indicated by the moment tensor solutions with the black dashed boxes showing the rupture zones (Chen et al., 2004; Bennington et al., 2011). The epicenters of local earthquakes listed in the USGS NCSN catalog from 2000/01/01 to 2012/02/27 (http://www.ncedc.org) are indicated by the small grey dots. The large blue, green, red and black circles show the locations of low-frequency earthquake (LFE) families in categories 1–4, respectively, with the filled circles indicating those families with long-term recovery (LTR) in LFE recurrence after the Parkfield earthquake, and the open circles showing those families without clear LTR. The colored numbers by the side of some LFE families indicate the family IDs. The white triangles show the locations of the HRSN stations, and the green triangles show the locations of the NCSN stations. The black lines indicate active faults and the brown squares indicate the geographical locations in this region. The two red dashed lines define the 3 sub-regions of the northeast, along the San Andreas fault (SAF), and southwest around the San Simeon earthquake epicenter. The inset is a map of California with the red box showing the region plotted in the main map. (b) Cross-section view along the SAF. The black and red stars indicate the 1966 and 2004 Parkfield earthquake hypocenter, respectively. The hypocenters of regular earthquakes in Region 2 are indicated by the small grey dots. The large circles with different colors show the locations of the LFEs in different categories. The vertical black dashed line indicates the boundary between the Northern and Southern LFE families. The other symbols are the same as in panel (a). (For interpretation of the references to color in this figure legend, the reader is referred to the web version of this article.)

Here we examine catalogs spanning ~12 yr of earthquakes and LFEs in the Parkfield region, to investigate the long-term temporal changes in earthquake and LFE inter-event times (IET) and LFE recurrence times after the San Simeon and Parkfield earthquakes. Note that IET refers to the time between successive failures of the same or different fault segments, but LFE recurrence time refers to time between recurring ruptures of the same fault segment. We use IET to track the general temporal evolution of seismic activities and LFE recurrence time to track the more localized temporal changes in the deeper crust. We show long-term recovery after the San Simeon and Parkfield earthquakes and discuss several possible causative mechanisms.

## 2. Data and analysis procedure

### 2.1. Earthquake and LFE catalogs

For the regular earthquakes, we utilize the Northern California Seismic Network (NCSN) catalog from 2000 to 2012. We select the earthquakes within a region bounded by 121.2°W to 119.9°W and 35.3°N to 36.6°N (Fig. 1a), resulting in a catalog of ~50,000 earthquakes. Depths range from 0 to ~100 km, with 99.6% of the earthquakes shallower than 20 km, and magnitudes range from −0.22 to 5.0, except for the Mw6.5 San Simeon and the Mw6.0 Parkfield earthquakes. The magnitude of completeness ($M_C$) of the NCSN catalog depends on location and time, and is generally between ~1 and 1.5 (e.g., Schorlemmer et al., 2004; Woessner and Wiemer, 2005) except during the periods immediately after local large earthquakes (e.g., after the 2004 Parkfield earthquake, Peng et al., 2006; Peng and Zhao, 2009). Additional details on the earthquake catalog can be found at the NCSN website (http://www.ncedc.org/ncsn/).

For the LFEs, we utilize the updated LFE catalog from 2001 to 2012, in which LFE families (groups of repeated similar events) are located using *P*- and *S*-wave arrivals measured from stacked seismic waveforms (Shelly and Hardebeck, 2010). Repeated occurrences of similar LFEs are identified by cross-correlation of the LFE family template waveforms with the continuous seismic data at multiple HRSN stations (Shelly et al., 2009). The locations of the 88 LFE families (with a total of ~730,000 LFEs) used in this study are shown in Fig. 1. The depths of the LFE families range from ~16 to 30 km, and their estimated moment magnitudes are typically $<0.5$ (e.g., Nadeau and Dolenc, 2005).

### 2.2. Analysis procedure

For the earthquakes, we divide our study region into three sub-regions to separate the effects of the 2003 San Simeon and 2004 Parkfield earthquakes. Region 2 contains the creeping and locked Parkfield–Cholame sections of the San Andreas fault (SAF), including the segment that ruptured during the 2004 Parkfield earthquake. Region 1 is northeast of this and Region 3 to the southwest, including the rupture zone of the 2003 San Simeon earthquake (Fig. 1a). Region 1 is used as a reference as it is relatively far from both the Parkfield and San Simeon earthquakes and assumed to be relatively unaffected by the static stress changes from both earthquakes. For each sub-region, we first select earthquakes with magnitude above the magnitude of completeness ($M_C$=~1.5). Then we compute IETs between temporally adjacent earthquakes (Fig. S1). We use an inter-event time approach that does not rely on the time bin size traditionally used to compute the seismicity rate. We focus on the long-term (months to years) temporal changes in the earthquake IETs before and after the Parkfield earthquake in Regions 1 and 2, and before and after the San Simeon earthquake for Region 3. We estimate the reference IET for each sub-region by computing the arithmetic average of all the IETs in each sub-region before the San Simeon earthquake. We use logarithmic instead of linear time in the post-seismic periods so that each time bin contains similar numbers of IETs due to the power law decay of aftershocks (Omori, 1894). Next, we compute the average IET in each of the time bins for the three sub-regions,

respectively. We use a bin size of 0.25 log(s), and verified that results are stable for time windows varying from 0.1 to 0.4. Finally we estimate the recovery time when 90% of the co-seismic IET drop is recovered.

Due to the complexity in the LFE recurrence (Shelly, 2010b), we group the 88 LFE families into 4 categories, separating them subjectively according to the distribution of recurrence times: (1) bi-modal (Fig. S2a), (2) tri-modal (Fig. S2b), (3) period-doubling (Fig. S2c), and (4) chaotic families (Fig. S2d). In the period-doubling cases, the band of longer recurrence intervals concentrate at ~3 and ~6 days. We mainly focus on the first two categories because the period-doubling families have been analyzed in detail by Shelly (2010b) and the recurrence times in the chaotic families show no clear change after the Parkfield earthquake in this analysis. We analyze each of the recurrence bands (i.e., recurrence time in certain ranges) separately for LFE families in categories 1 and 2. The boundaries of each recurrence band are initially determined by eye after inspecting the data after 2008 when the recurrence times are mostly recovered from the influence of the Parkfield earthquake. Then we test the robustness of the boundaries by varying them in a small range and repeat the analysis. We only considered families that have behaviors that do not depend on these boundaries. For 67 of the 88 LFE families, we treat the pre- and post-Parkfield-earthquake recurrence times in each LFE family in the same way as for the earthquakes. As mentioned before, in this study we focus primarily on the long-term temporal changes of LFE recurrence after the Parkfield earthquake because previous studies have investigated shorter-term changes in detail (Nadeau and Guilhem, 2009; Shelly and Johnson, 2011).

## 3. Results

### 3.1. Earthquake IET

We first examine qualitatively effects of both the San Simeon and Parkfield earthquakes based on un-stacked IETs as a function of linear time, because some details could be lost in the averaging procedure. In Region 1 northeast of the SAF, there are only ~3500 earthquakes from 2000 to 2012. As shown in Fig. S1a, there are sporadic drops in the IET due to the aftershocks of local earthquakes, but there is no clear change in the IET after the San Simeon or Parkfield earthquake. In Region 2 along the SAF, there are ~25,000 earthquakes. There is a clear drop in the earthquake IET after the 2004 Parkfield earthquake. The IETs gradually recover to the pre-Parkfield earthquake value after several years. There is no clear effect of the San Simeon earthquake on the IETs in the Region 2 (Fig. S1b). In Region 3 southwest of the SAF, there are ~21,000 earthquakes. The IETs drop dramatically after the San Simeon earthquake and start to recover afterwards, and still have not recovered to the pre-San Simeon earthquake value as of 2012. There is no obvious effect of the Parkfield earthquake on the IET in this region (Fig. S1c).

Fig. 2 shows the averaged IETs versus the logarithmic times since the San Simeon (Region 3) and Parkfield (Regions 1 and 2), respectively. In Region 1 northeast of the SAF, the averaged IETs do not change significantly after the Parkfield earthquake (Fig. 2a). In Region 2 along the SAF, the IETs drop from the background value of ~$10^{4.5}$ s to less than 100 s after the Parkfield earthquake, and then gradually recover to the pre-Parkfield earthquake value after ~$10^{8}$ s or ~3 yr (Fig. 2b). In Region 3 southwest of the SAF, the IETs drop from ~$10^{5.5}$ s to less than 100 s after the San Simeon earthquake (Fig. 2c), and then gradually recover to ~$10^{5}$ s as of February 2012 (~8 yr after the San Simeon earthquake, Fig. 2c).

### 3.2. LFE IET and recurrence

We first examine the general pattern of the LFE IET from the entire LFE catalog with all the families combined as a comparison to the regular earthquake IET. As shown in Fig. 3, there is a general decrease in the maximum LFE IETs for the northern (Fig. 1b), southern (Fig. 1b), and all the families after the Parkfield earthquake, and the decrease lasts for at least several years. Then we examine the LFE recurrence times within each individual LFE family. After categorizing the LFE families by their recurrence patterns, we have 48 families in the category 1 (bi-modal recurrence), 19 families in category 2 (tri-modal recurrence), 4 families in category 3 (period-doubling), and 17 families in category 4 (chaotic). After averaging the recurrence times in different time periods after the Parkfield earthquake for category 1 and 2 LFE families (i.e., Fig. 4), we observed a clear drop and long-term recovery for 19 of 48 families in category 1 (blue circles in Fig. 1) and 8 of 19 families in category 2 (green circles in Fig. 1). The drop and recovery pattern is more evident in longer recurrence bands, which recover on time scales of ~$10^{7}$–$10^{8}$ s or ~4 months to several years (e.g., Fig. 4). Note that the co-seismic drop of the higher mode recurrence times for most of the category 1 and 2 LFE families hardly exceeds one standard deviation of the reference value (e.g., Fig. 4, Fig. S3).

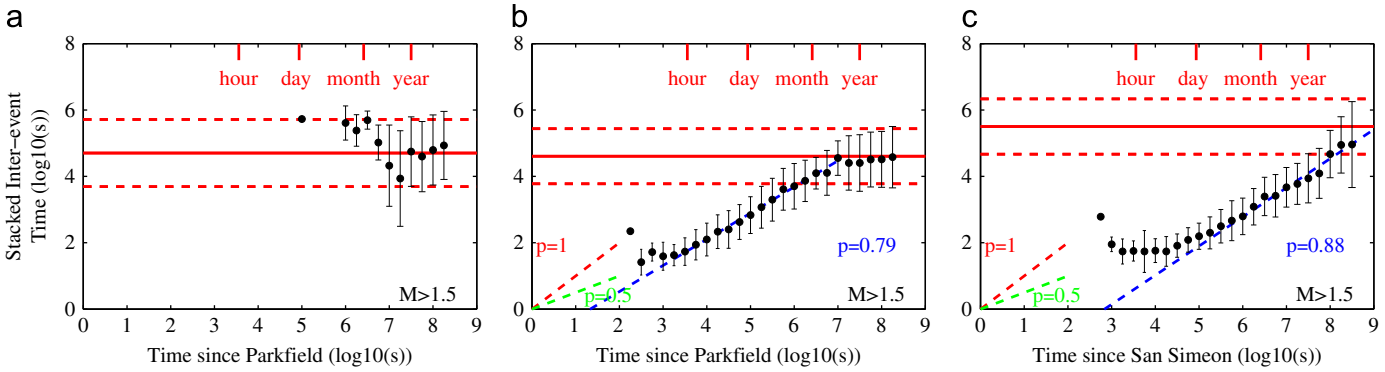


**Fig. 2.** (a) Time-binned IETs of earthquakes with magnitude above the magnitude of completeness ($M_C$=~1.5) plotted against time since the 2004 Parkfield earthquake for Region 1 northeast of the SAF. Both the averaged IET (*Y*-axis) and the elapse time after the Parkfield earthquake (*X*-axis) are in logarithmic scales. The black dots with error bars indicate the averaged IET and one standard deviation for each 0.25 logarithmic time bin. The red horizontal solid and dashed lines indicate the reference IET averaged from all the events from 2000/01/01 to the occurrence time of 2003 San Simeon earthquake (2003/12/22) and the standard deviation, respectively. (b) Similar figure as (a) for Region 2 along the SAF. The blue dashed line shows the first order least squares fitting of the data from ~$10^{5.5}$ to $10^{7}$ s. The green and red dashed lines show the reference rates with $p$=0.5 and 1. (c) Similar figure as (a) for Region 3 southwest of the SAF. The *X*-axis is the lapse time in logarithmic scale after the San Simeon earthquake. The blue dashed line shows the first order least squares fitting of the data from ~$10^{6}$ to $10^{8.5}$ s. The green and red dashed lines show the reference rates with $p$=0.5 and 1. (For interpretation of the references to color in this figure legend, the reader is referred to the web version of this article.)

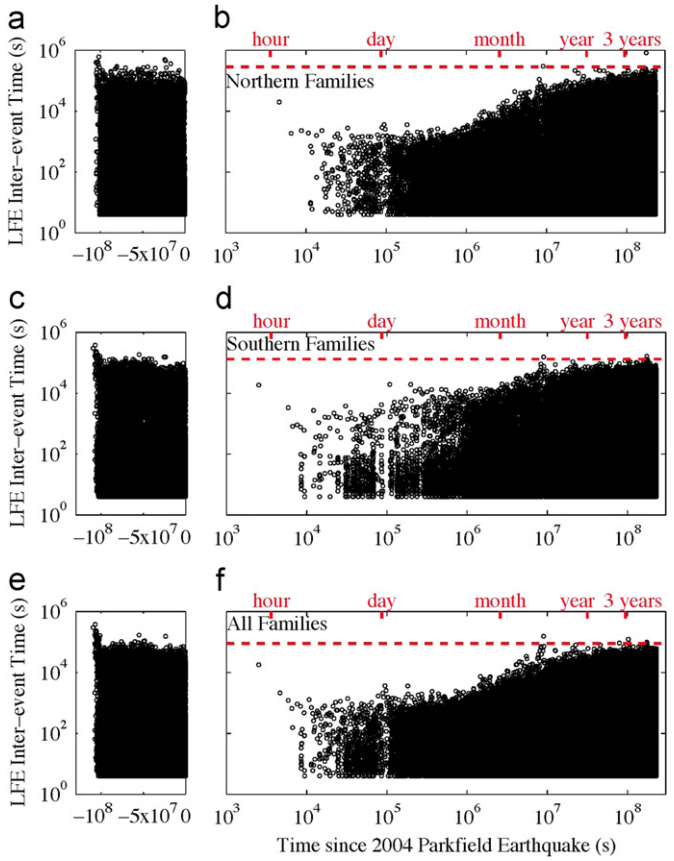


**Fig. 3.** (a–b) LFE IET computed from the LFE catalog with all the Northern LFE families combined (a) before and (b) after the Parkfield earthquake. The initial drop in the maximum LFE IET before the Parkfield earthquake is due to the HRSN gain changes. The horizontal red line indicates the 99.99% level of IET between the HRSN gain changes and the San Simeon Earthquake. The red ticks at the top mark time scales of 1 h, 1 day, 1 month, 1 yr, and 3 yr. Note that the *X*-axis is in linear scale in (a) and logarithmic scale in (b). (c–d) Similar figures as (a–b) for the LFE catalog with all the Southern LFE families combined. (e–f) Similar figures as (a–b) for the lFE catalog with all the LFE families combined. (For interpretation of the references to color in this figure legend, the reader is referred to the web version of this article.)

To verify the changes in the recurrence times after the Parkfield earthquake, we compared the probability density distribution of the recurrence times before the San Simeon earthquake and in the 2-month period after the Parkfield earthquake (Fig. S4). As shown in Fig. S4, the distribution of recurrence times after the Parkfield earthquake is quite different from the one before the San Simeon earthquake, with the higher mode peaks shifted to lower values. For the category 3 LFE families, the two higher bands are perturbed by the Parkfield earthquake but cannot be analyzed separately as they overlap with each other after the Parkfield main shock (Fig. S5). We inspected the category 3 LFE families by eye and found 3 out of 4 of them show clear long-term recovery in the two higher bands (Fig. S5, red circles in Fig. 1). We did not observe clear long-term recovery in the recurrence times for the LFE family 16 in category 3 (Fig. S5b) due to large uncertainties, and for the category 4 LFE families (e.g., Fig. S2d, black open circles in Fig. 1). It appears that most of the LFE families in categories 1 and 2 with clear long-term recovery after the Parkfield earthquake are clustered at two distinct locations both at ~20–25 km depth close to the Parkfield earthquake rupture: beneath the 2004 Parkfield earthquake hypocenter and immediately north of the hypocenter of the 1966 Mw6.0 Parkfield earthquake. However, there are also several category 1 and 2 LFE families close to these two locations that do not show clear long-term recovery in recurrence interval statistics (blue and green open circles in Fig. 1).

## 4. Discussion

We observed long-term changes in earthquake IETs in the region along the SAF after the 2004 Parkfield earthquake and in the region to the southwest region after the 2003 San Simeon earthquake, respectively (Fig. 2). The long-term recovery of earthquake IET largely reflects the temporal pattern of aftershock sequences triggered directly and indirectly by the two large main shocks (Helmstetter and Sornette, 2002). Previous studies on aftershock statistics generally suggest that large shallow earthquakes are typically followed by aftershocks that decay in rate approximately as the inverse of the elapsed time since the main shock, as described by the modified Omori's law (Utsu et al., 1995):

$$R(t) = \frac{K}{(t+c)^p}, \tag{1}$$

where $R(t)$ is the aftershock rate, $K$ is the aftershock productivity, $t$ is the elapsed time since the main shock, $p$ is the region specific slope of power law decay, and $c$ is the time delay before the onset of the aftershock decay. As shown in Fig. S6, the aftershock rate in Region 2 generally follows the power law decay as described by the modified Omori's law. The $p$ value estimated from $M > 1.5$ (above $M_C$ of ~1–1.5) between about three days to three months after the Parkfield earthquake with relatively complete aftershock records is ~0.80 (Fig. S6). As the IET is inversely proportional to the seismicity rate, Eq. (1) could be rewritten as

$$\log T(t) = p \log(t+c) - \log(K) \tag{2}$$

where $T(t)$ is the IET, and other symbols are the same as in Eq. (1). Eq. (2) roughly describes the long-term recovery of earthquake IET we observed after the Parkfield and San Simeon earthquakes, except for the earlier periods (Fig. 2). The $p$ value is ~0.79 if we consider only earthquakes from about 10 days to three months after the Parkfield earthquake (Fig. 2b), and the $p$ value estimated from about one month to eight years after the San Simeon earthquake is ~0.88 (Fig. 2c).

To overcome biases caused by missing early aftershocks, we merge an early aftershock catalog developed by Peng and Zhao (2009) into the NCSN catalog containing ~15,000 events in region 2 from 100 s to 3 days after the Parkfield earthquake. As shown in Fig. S7, the IET during the 100 s to 3 days period after the Parkfield earthquake is significantly shortened after adding the missing aftershocks. However, there is a jump at the ending time of the early aftershock catalog, indicating that aftershocks are still missing in the NCSN catalog. A more complete early aftershock catalog is not available for the San Simeon earthquake so we could not apply the same procedure to Region 3. Due to the missing aftershocks in the catalog, the observed co-seismic drop in the earthquake IET is probably underestimated.

The observed time scale of IET recovery is ~3 yr for Region 2 and more than 8 yr for Region 3, respectively. As the IET recovery is consistent with being a typical aftershock sequence, our observation suggests that the aftershock sequence duration for the San Simeon earthquake is much longer than that for the Parkfield earthquake. Previous studies have proposed that aftershock sequence duration is proportional to main shock recurrence time (Dieterich, 1994), and inversely proportional to the fault loading rate (Stein and Liu, 2009). The observation here is consistent with their hypothesis, as the loading rate of ~25–30 mm/yr at the Parkfield section of SAF is believed to be much higher than the loading rate of $< 5$ mm/yr at the Oceanic fault, the thrust fault on which the San Simeon earthquake occurred (Argus and Gordon,

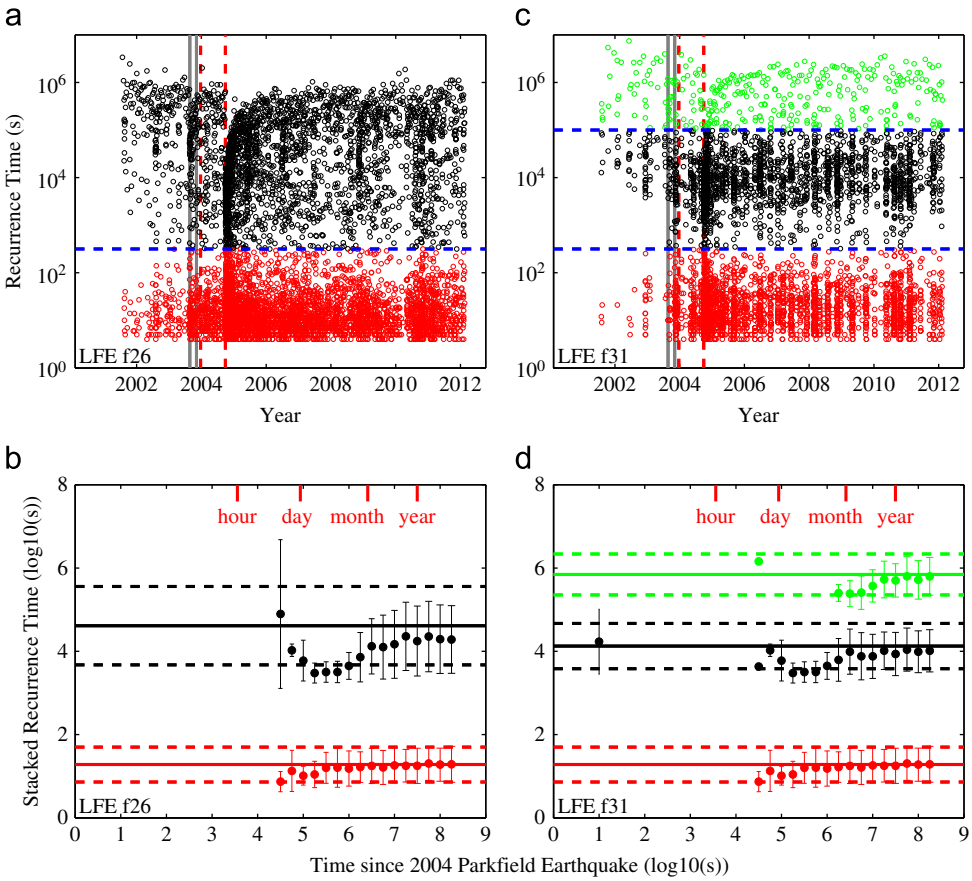


**Fig. 4.** (a) Recurrence times for LFE family 26 plotted against their occurrence times. The two vertical red dashed lines indicate the occurrence times of the 2003 San Simeon and 2004 Parkfield earthquakes. The two vertical grey lines indicate the HRSN network gain changes. The horizontal blue dashed line shows the boundary of the higher and lower recurrence bands. The recurrence times in the higher and lower bands are shown in black and red dots, respectively. (b) Time-binned recurrence time of LFE family 26. Both the stacked recurrence time (*Y*-axis) and the elapse time after the Parkfield earthquake (*X*-axis) are in logarithmic scales. The black and red dots with error bars indicate the stacked recurrence time and standard deviation in each 0.25 logarithmic time bin for the higher and lower mode, respectively. The black horizontal solid and dashed lines indicate the reference recurrence time for the higher mode averaged from all the events from 2001 to the occurrence time of 2003 San Simeon earthquake (2003/12/22) and the standard deviation, respectively. The red horizontal solid and dashed lines indicate the reference recurrence time for the lower mode and the standard deviation, respectively. The red ticks at the top mark time scales of 1 h, 1 day, 1 month, and 1 yr. (c–d) Similar figures as (a–b) for LFE family 31. (For interpretation of the references to color in this figure legend, the reader is referred to the web version of this article.)

2001; Hardebeck et al., 2004; Murray and Langbein, 2006; McLaren et al., 2008). This is consistent with previous studies of historic earthquakes that have shown that the aftershock duration varies in different tectonic settings and correlates with the fault loading rate (Stein and Liu, 2009). Previous studies have suggested that the aftershocks of the Parkfield earthquake are largely driven by afterslip (e.g., Langbein et al., 2006; Freed, 2007; Barbot et al., 2009). The post-seismic moment release of the San Simeon earthquake is only ~14% of the co-seismic slip (Johanson and Burgmann, 2010). In addition, the size of the San Simeon earthquake is larger than the Parkfield earthquake. So the differences in size and afterslip between Parkfield and San Simeon earthquakes could also influence the aftershock sequence and duration.

Previous studies have demonstrated that tremor activity and LFE rates increased sharply after the Parkfield earthquake (Nadeau and Guilhem, 2009; Shelly, 2010a; Shelly and Johnson, 2011; Guilhem and Nadeau, 2012). Specifically, Nadeau and Guilhem (2009) found that tremor activity increased and remained elevated for over 4 yr after the Parkfield earthquake. Shelly and Johnson (2011) found increases up to 1–2 orders of magnitude in LFE rate that peaked at a few days after the Parkfield earthquake, and the rate remain elevated for more than a year for some of the LFE families. Guilhem and Nadeau (2012) found that the recurrence interval of the largest tremor episodes become regular after the Parkfield earthquake and gradually evolve from ~60 days to ~120 days from 2005 to 2008, and then become irregular again. In this study, we observe a decrease in the higher mode of LFE recurrence times to a minimum of ~$10^5$ s or ~1 day after the Parkfield earthquake, followed by a recovery of ~$10^7$–$10^8$ s or ~4 months to several years for some of the LFE families (e.g., Figs. 4 and S3). The recurrence pattern of some LFE families (e.g., Fig. S2d) show similar episodic pattern as the tremor activities shown in Guilhem and Nadeau (2012). Our results are generally consistent with that of Shelly and Johnson (2011) and Guilhem and Nadeau (2012), but further suggest a long-term recovery of LFE recurrence after the Parkfield earthquake (Fig. 4). The advantage of using recurrence time as a probe of the LFE activities is that different recurrence bands can be analyzed separately. However, we note that some LFE families showing clear increase in the LFE event rate after the Parkfield earthquake (Shelly and Johnson, 2011) do not show clear long-term recovery pattern (open circles in Fig. 1) in LFE recurrence analysis in this study. We checked the recurrence pattern of these LFE families and found that they are either category 4 (chaotic) families or category 1 and 2 families with relatively large uncertainties in the LFE recurrence time. Hence, we cannot rule out the possibility that long-term recovery of LFE recurrence time exists for some LFE families but is masked by the relatively large uncertainties in these families.

The drop and recovery in the longer recurrence bands of the LFE observations in this study (Fig. 4) suggest that Parkfield

earthquake could have increased the rate of deep fault creep. According to Shelly (2010b), the longer recurrence times of the bi-modal LFE families and the middle mode of the tri-modal families are likely sources that are loaded in a mostly steady fashion by surrounding fault creep. He also suggests that the shortest recurrence times in both types of families reflect failure of overlapping sources as driving slip migrations, while the longest tri-modal mode corresponds to the failures between slow slip events. Johnson et al. (2012) observed similar bi-modal recurrence of triggered slow slip events simulated in laboratory, and inferred the lower mode corresponded to individual slip events within a major slip event, and the higher mode to the time between major slip events. We are unable to resolve any clear changes in the shortest recurrence band (Fig. 4).

As proposed in previous studies, the drop in the LFE recurrence time is likely to be mainly caused by the positive static stress and possibly dynamic stress induced by the Parkfield earthquake (Nadeau and Guilhem, 2009; Shelly and Johnson, 2011). The initial gradual drop of the LFE recurrence time could be due to the fact that the LFE detection is inhibited during the first day after the Parkfield earthquake or potential propagation of the afterslip from the Parkfield earthquake source region to the LFE source region (Shelly and Johnson, 2011). The long-term recovery may reflect the process of the post-seismic relaxation of the positive static stress by the deep fault creep (Shelly and Johnson, 2011), or gradual recovery of the fault zone friction properties altered by dynamic or quasi-static loading (Dieterich, 1994; Johnson and Jia, 2005; Brenguier et al., 2008). The roles of the two mechanisms cannot be distinguished by the observations here, but will be investigated in a follow-up study by modeling the recurrence time of LFE with different applied stress and friction parameters (e.g., Daub et al., 2011). Possible causes for the diversity in recovery time (~4 month to several years) for different LFE families includes: (1) variations in static stress induced by the Parkfield earthquake and its afterslip, (2) variable loading rate, and (3) variation in deep fault friction properties at different LFE family locations (Lengline and Marsan, 2009; Shelly, 2010a,b; Shelly and Johnson, 2011). These mechanisms should be tested in future studies.

Chen et al. (2010) found that the recurrence time of repeating earthquakes in the Parkfield region decreased after the Parkfield earthquake and recovered over ~4 yr, which is comparable to the recovery time scale of the earthquake IET in Region 2 (~3 yr), and the recovery time scale of LFE recurrence (~4 month to several years) in this study. The fact that the recovery time scale for a single fault patch at seismogenic depth (repeating earthquake recurrence time), a single fault patch in the lower crust (LFE recurrence time), and for multiple fault segments at the seismogenic depths (earthquake IET) are in the same order of magnitude indicates that they could be controlled by similar mechanisms (e.g., Lengline and Marsan, 2009; Peng and Gomberg, 2010). If true, this would suggest that earthquake IET and LFE recurrence time could provide important information regarding the overall loading and stressing physics of the fault system and associated volume. However, this hypothesis still needs to be tested further by more extensive datasets.

## Acknowledgments

This research was supported by Institutional Support at Los Alamos National Lab (CW and PJ), the USGS (DS and JG), and the National Science Foundation EAR-0956051 (ZP). We thank Jeanne Hardebeck, Justin Sweet, and two anonymous reviewers for their constructive review comments. We thank Robert Guyer, Eric Daub, Jan Carmeliet, Behrooz Fedowsi, Eli Ben-Naim, and Michele Griffa for discussions.

## Appendix A. Supporting information

Supplementary data associated with this article can be found in the online version at http://dx.doi.org/10.1016/j.epsl.2013.03.007.

## References

Argus, D.F., Gordon, R.G., 2001. Present tectonic motion across the Coast Ranges and San Andreas fault system in central California. Geol. Soc. Am. Bull. 113, 1580–1592.
Aron, A., Hardebeck, J.L., 2009. Seismicity rate changes along the central California coast due to stress changes from the 2003 M 6.5 San Simeon and 2004 M 6.0 Parkfield earthquakes. Bull. Seismol. Soc. Am. 99, 2280–2292.
Bakun, W., Aagaard, B., Dost, B., Ellsworth, W., Hardebeck, J., Harris, R., Ji, C., Johnston, M., Langbein, J., Lienkaemper, J., 2005. Implications for prediction and hazard assessment from the 2004 Parkfield earthquake. Nature 437, 969–974.
Barbot, S., Fialko, Y., Bock, Y., 2009. Postseismic deformation due to the Mw 6.0 2004 Parkfield earthquake: stress-driven creep on a fault with spatially variable rate-and-state friction parameters. J. Geophys. Res. 114, B07405.
Bennington, N., Thurber, C., Feigl, K.L., Murray-Moraleda, J., 2011. Aftershock distribution as a constraint on the geodetic model of coseismic slip for the 2004 Parkfield earthquake. Pure Appl. Geophys. 168, 1553–1565.
Brenguier, F., Campillo, M., Hadziioannou, C., Shapiro, N., Nadeau, R., Larose, E., 2008. Postseismic relaxation along the San Andreas fault at Parkfield from continuous seismological observations. Science 321, 1478.
Chao, K., Peng, Z., Wu, C., Tang, C.C., Lin, C.H., 2012. Remote triggering of non-volcanic tremor around Taiwan. Geophys. J. Int. 188, 301–324.
Chen, J., Larson, K.M., Tan, Y., Hudnut, K.W., Choi, K., 2004. Slip history of the 2003 San Simeon earthquake constrained by combining 1-Hz GPS, strong motion, and teleseismic data. Geophys. Res. Lett. 31, L17608.
Chen, K.H., Burgmann, R., Nadeau, R.M., Chen, T., Lapusta, N., 2010. Postseismic variations in seismic moment and recurrence interval of repeating earthquakes. Earth Planet. Sci. Lett. 299, 118–125.
Daub, E.G., Shelly, D.R., Guyer, R.A., Johnson, P.A., 2011. Brittle and ductile friction and the physics of tectonic tremor. Geophys. Res. Lett. 38, L10301.
Dieterich, J., 1994. A constitutive law for rate of earthquake production and its application to earthquake clustering. J. Geophys. Res. 99, 2601–2618.
Freed, A.M., 2007. Afterslip (and only afterslip) following the 2004 Parkfield, California, earthquake. Geophys. Res. Lett. 34, L06312.
Gomberg, J., Rubinstein, J., Peng, Z., Creager, K., Vidale, J., Bodin, P., 2008. Widespread triggering of nonvolcanic tremor in California. Science 319, 173.
Guilhem, A., Nadeau, R.M., 2012. Episodic tremors and deep slow-slip events in Central California. Earth Planet. Sci. Lett. 357, 1–10.
Hardebeck, J.L., Boatwright, J., Dreger, D., Goel, R., Graizer, V., Hudnut, K., Ji, C., Jones, L., Langbein, J., Lin, J., 2004. Preliminary report on the 22 December 2003, M 6.5 San Simeon, California earthquake. Seismol. Res. Lett. 75, 155–172.
Helmstetter, A., Sornette, D., 2002. Diffusion of epicenters of earthquake aftershocks, Omori's law, and generalized continuous-time random walk models. Phys. Rev. E 66, 061104.
Hill, D., Prejean, S., 2007. Dynamic triggering. In: Kanamori, H. (Ed.), Earthquake Seismology Treatise on Geophysics. Elsevier, Amsterdam, pp. 257–291.
Johanson, I., Burgmann, R., 2010. Coseismic and postseismic slip from the 2003 San Simeon earthquake and their effects on backthrust slip and the 2004 Parkfield earthquake. J. Geophys. Res. 115, B07411.
Johnson, P., Carpenter, B., Knuth, M., Kaproth, B., Le Bas, P.Y., Daub, E., Marone, C., 2012. Nonlinear dynamical triggering of slow slip on simulated earthquake faults with implications to Earth. J. Geophys. Res. 117, B04310.
Johnson, P., Jia, X., 2005. Nonlinear dynamics, granular media and dynamic earthquake triggering. Nature 437, 871–874.
Langbein, J., Murray, J., Snyder, H., 2006. Coseismic and initial postseismic deformation from the 2004 Parkfield, California, earthquake, observed by Global Positioning System, electronic distance meter, creepmeters, and borehole strainmeters. Bull. Seismol. Soc. Am. 96, S304–S320.
Lengline, O., Marsan, D., 2009. Inferring the coseismic and postseismic stress changes caused by the 2004 Mw=6 Parkfield earthquake from variations of recurrence times of microearthquakes. J. Geophys. Res. 114, B10303.
McLaren, M.K., Hardebeck, J.L., van der Elst, N., Unruh, J.R., Bawden, G.W., Blair, J.L., 2008. Complex faulting associated with the 22 December 2003 MW 6.5 San Simeon, California, earthquake, aftershocks, and postseismic surface deformation. Bull. Seismol. Soc. Am. 98, 1659–1680.
Murray, J., Langbein, J., 2006. Slip on the San Andreas fault at Parkfield, California, over two earthquake cycles, and the implications for seismic hazard. Bull. Seismol. Soc. Am. 96, S283–S303.
Nadeau, R.M., Dolenc, D., 2005. Nonvolcanic tremors deep beneath the San Andreas fault. Science 307, 389.
Nadeau, R.M., Guilhem, A., 2009. Nonvolcanic tremor evolution and the San Simeon and Parkfield, California, earthquakes. Science 325, 191–193.
Omori, F., 1894. On the after-shocks of earthquakes. J. Coll. Sci. Imp. Univ. Tokyo 7, 111–200.
Peng, Z., Gomberg, J., 2010. An integrated perspective of the continuum between earthquakes and slow-slip phenomena. Nat. Geosci. 3, 599–607.

Peng, Z., Vidale, J., Houston, H., 2006. Anomalous early aftershock decay rate of the 2004 Mw6. 0 Parkfield, California, earthquake. Geophys. Res. Lett. 33, L17307.
Peng, Z., Vidale, J., Wech, A., Nadeau, R., Creager, K., 2009. Remote triggering of tremor along the San Andreas Fault in central California. J. Geophys. Res. 114, B00A06, http://dx.doi.org/10.1029/2008JB006049.
Peng, Z., Zhao, P., 2009. Migration of early aftershocks following the 2004 Parkfield earthquake. Nat. Geosci. 2, 877–881.
Rubinstein, J.L., Shelly D.R., Ellsworth W.L., 2010. Non-volcanic tremor: a window into the roots of fault zones. In: Cloetingh, S., and Negendank, J. (Eds.) New Frontiers in Integrated Solid Earth Sciences, Springer, Dordrecht, Netherlands, pp. 287-314.
Schorlemmer, D., Wiemer, S., Wyss, M., 2004. Earthquake statistics at Parkfield: 1. Stationarity of b values. J. Geophys. Res. 109, B12307.
Shelly, D., Peng, Z., Hill, D.P., Aiken, C., 2011. Tremor evidence for dynamically triggered creep events on the deep San Andreas Fault. Nat. Geosci. 4, 384–388.
Shelly, D.R., 2009. Possible deep fault slip preceding the 2004 Parkfield earthquake, inferred from detailed observations of tectonic tremor. Geophys. Res. Lett. 36, L17318.
Shelly, D.R., 2010a. Migrating tremors illuminate complex deformation beneath the seismogenic San Andreas fault. Nature 463, 648–652.
Shelly, D.R., 2010b. Periodic, chaotic, and doubled earthquake recurrence intervals on the deep San Andreas Fault. Science 328, 1385–1388.
Shelly, D.R., Beroza, G.C., Ide, S., 2007. Non-volcanic tremor and low-frequency earthquake swarms. Nature 446, 305–307.
Shelly, D.R., Ellsworth, W.L., Ryberg, T., Haberland, C., Fuis, G.S., Murphy, J., Nadeau, R.M., Burgemann, R., 2009. Precise location of San Andreas Fault tremors near Cholame, California using seismometer clusters: slip on the deep extension of the fault? Geophys. Res. Lett. 36, L01303.
Shelly, D.R., Hardebeck, J.L., 2010. Precise tremor source locations and amplitude variations along the lower-crustal central San Andreas Fault. Geophys. Res. Lett. 37, L14301.
Shelly, D.R., Johnson, K.M., 2011. Tremor reveals stress shadowing, deep postseismic creep, and depth-dependent slip recurrence on the lower-crustal San Andreas fault near Parkfield. Geophys. Res. Lett. 38, L13312.
Stein, R.S., 1999. The role of stress transfer in earthquake occurrence. Nature 402, 605–609.
Stein, S., Liu, M., 2009. Long aftershock sequences within continents and implications for earthquake hazard assessment. Nature 462, 87–89.
Utsu, T., Ogata, Y., Matsu'ura, R.S., 1995. The centenary of the Omori formula for a decay law of aftershock activity. J. Phys. Earth 43, 1–33.
Woessner, J., Wiemer, S., 2005. Assessing the quality of earthquake catalogues: estimating the magnitude of completeness and its uncertainty. Bull. Seismol. Soc. Am. 95, 684–698.